Scientific paper

Synthesis, Spectroscopic Characterization, Crystal Structures and Antibacterial Activity of Vanadium(V) Complexes of Fluoro- and Chloro-Substituted Benzohydrazone Ligands

En-Cheng Liu,[1] Wei Li[1,*] and Xiao-Shan Cheng[2]

[1] *Department of Radiology, The Second Hospital of Dalian Medical University, Dalian 116023, P.R. China*

[2] *Department of Chemistry and Chemical Engineering, Liaoning Normal University, Dalian 116029, P. R. China*

** Corresponding author: E-mail: liwei_dlmu@126.com, youzhonglu@126.com*

Received: 04-25-2019

Abstract

A new vanadium(V) complex, [VOL(OMe)(MeOH)]·MeOH (**1**·MeOH), was prepared by the reaction of $VO(acac)_2$ with 2-chloro-*N*'-(5-fluoro-2-hydroxybenzylidene)benzohydrazide (H_2L) in methanol. By addition of salicylhydroxamic acid (HSHA) to the methanolic solution of **1**, a new salicylhydroxamate-coordinated vanadium(V) complex, [VOL(SHA)]·H_2O (**2**·H_2O), was obtained. Both complexes were characterized by elemental analysis, infrared spectroscopy, thermal analysis and single crystal X-ray diffraction. Complex **1** crystallizes with methanol molecule as a solvate, and complex **2** as a monohydrate. The V atoms in the complexes are in octahedral coordination. In the crystal structure of **1**·MeOH, the vanadium complexes are linked by methanol solvate molecules through intermolecular O–H···N and O–H···O hydrogen bonds to form chains along the *c* axis. In the crystal structure of **2**·H_2O, the vanadium complexes are linked by water molecules through intermolecular O–H···O hydrogen bonds, to form 1D chains along the *a* axis. The chains are further linked through intermolecular O–H···N and O–H···O hydrogen bonds in the *c* direction to form 2D layers. The antimicrobial activities of the complexes against *K. pneumoniae*, *S. aureus*, *P. aeroginosa*, *E. coli*, and *B. subtilis* were investigated.

Keywords: Hydrazone ligand; Salicylhdroxamate ligand; Vanadium complex; Crystal structure; Antibacterial activity.

1. Introduction

In recent years, vanadium complexes have been reported to have interesting biological activities such as normalizing the high blood glucose levels and acting as models of haloperoxidases.[1] Hydrazone compounds derived from the condensation reaction of aldehydes with various hydrazides are much attractive for their structures, coordinate ability to metal atoms and extensive biological applications.[2] Recently, our research group has reported a few vanadium complexes with hydrazone ligands and their biological activities.[3] In general, V atom is readily adopt octahedral coordination. Hydrazone ligands can coordinate to the V atoms through three donor atoms. The remaining three positions of the octahedral coordination are usually occupied by one oxo oxygen and two solvent molecules, one with deprotonated and the other one neutral.[3a,4] The two solvent ligands are not coordinate so strong to the V atom that they are readily substituted by bidentate ligands, such as benzohydroxamate,[5] propane-1,3-diol-2-olate or propan-1-ol-3-olate,[6] 2-hydroxyethanolate,[7] *etc.* Salicylhydroxamic acid is a bidentate ligand, but very few examples of vanadium(V) complexes with this ligand have been reported. Fluoro- and chloro-substituted compounds are reported to have effective antibacte-

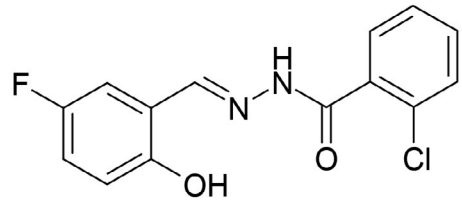

Scheme 1. H_2L

rial activities.[8] In the present paper, a new methanol and methoxy-coordinated vanadium(V) complex, [VOL(OMe)(MeOH)]·MeOH (**1**) and a salicylhydroxamate (SHA) coordinated vanadium(V) complex, [VOL(SHA)]·H_2O (**2**), where H_2L = 2-chloro-*N*'-(5-fluoro-2-hydroxybenzylidene)benzohydrazide (Scheme 1), are presented and studied on their antibacterial activities.

2. Experimental

2. 1. Materials and Measurements

Commercially available 5-fluorosalicylaldehyde, 2-chlorobenzohydrazide and salicylhyroxamic acid were purchased from Sigma-Aldrich and used without further purification. Other solvents and reagents were made in China and used as received. C, H and N elemental analyses were performed with a Perkin-Elmer elemental analyser. Infrared spectra were recorded on a Nicolet AVATAR 360 spectrometer as KBr pellets in the 4000–400 cm^{-1} region. Thermal stability analysis was performed on a Perkin-Elmer Diamond TG-DTA thermal analyses system. NMR spectra were recorded on a Bruker 500 MHz instrument.

2. 2. Synthesis of H_2L

5-Fluorosalicylaldehyde (1.0 mmol, 0.14 g) and 2-chlorobenzohydrazide (1.0 mmol, 0.17 g) were dissolved in methanol (30 mL) with stirring. The mixture was stirred for about 30 min at room temperature to give a clear solution. The solvent was evaporated to give colorless crystalline products. Yield, 96%. Analysis: Found: C 57.6%, H 3.5%, N 9.5%. Calculated for $C_{14}H_{10}ClFN_2O_2$: C 57.4%, H 3.4%, N 9.6%. IR data (KBr, cm^{-1}): ν 3372 (w, OH), 3232 (w, NH), 1651 (s, C=O), 1619 (s, C=N). UV-Vis (MeOH, nm): λ 225, 289, 305, 330, 405. ^{1}H NMR (d^6-DMSO, ppm) δ 12.16 (s, 1H, OH), 10.77 (s, 1H, NH), 8.49 (s, 1H, CH=N), 7.61–7.42 (m, 5H, ArH), 7.17 (d, 1H, ArH), 7.03 (d, 1H, ArH). ^{13}C NMR (d^6-DMSO, ppm) δ 162.85, 156.78, 154.91, 146.62, 135.23, 132.08, 131.24, 130.02, 128.99, 127.60, 120.31, 120.25, 118.82, 114.13.

2. 3. Synthesis of [VOL(OMe)(MeOH)]·MeOH (1)

A methanolic solution (10 mL) of [$VO(acac)_2$] (0.1 mmol, 26.5 mg) was added to a methanolic solution (10 mL) of H_2L (0.1 mmol, 29.2 mg) with stirring. The mixture was stirred for 30 min at room temperature to give a brown solution. The resulting solution was allowed to stand in air for a few days. Brown block-shaped crystals suitable for X-ray single crystal diffraction were formed at the bottom of the vessel. The isolated products were washed three times with cold ethanol, and dried in air. Yield, 72%. Analysis: Found: C 44.9%, H 4.4%, N 6.2%. Calculated for $C_{17}H_{19}ClFN_2O_6V$: C 45.1%, H 4.2%, N 6.2%. IR data (KBr, cm^{-1}): ν 3437 (m, OH), 1607 (s, C=N), 981 (V=O). UV-Vis (MeOH, nm): λ 270, 325, 413. ^{1}H NMR (d^6-DMSO, ppm) δ 8.88 (s, 1H, CH=N), 7.83 (d, 1H, ArH), 7.61–7.20 (m, 5H, ArH), 6.94 (d, 1H, ArH), 5.26 (s, 3H, CH_3), 3.94 (s, 3H, CH_3). ^{13}C NMR (d^6-DMSO, ppm) δ 171.50, 160.25, 156.55, 154.68, 132.52, 132.25, 131.72, 131.35, 131.12, 127.60, 120.73, 118.19, 117.97, 117.78, 74.54, 49.07. ^{51}V NMR (d^6-DMSO, ppm) δ –555.

2. 4. Synthesis of [VOL(SHA)]·H_2O (2)

A methanolic solution (10 mL) of salicylhydroxamic acid (0.1 mmol, 15.3 mg) was added to a methanolic solution (10 mL) of **1** (0.1 mmol, 45.3 mg) with stirring. The mixture was stirred for 30 min at room temperature to give a deep brown solution. The resulting solution was allowed to stand in air for a few days. Brown block-shaped crystals suitable for X-ray single crystal diffraction were formed at the bottom of the vessel. The isolated products were washed three times with cold ethanol, and dried in air. Yield, 51%. Analysis: Found: C 47.7%, H 3.0%, N 7.8%. Calculated for $C_{21}H_{16}ClFN_3O_7V$: C 47.8%, H 3.1%, N 8.0%. IR data (KBr, cm^{-1}): ν 3454 (m, OH), 3278 (w, NH), 1607 (s, C=N), 979 (V=O). UV-Vis (MeOH, nm): λ 266, 327, 408. ^{1}H NMR (d^6-DMSO, ppm) δ 12.16 (s, 1H, OH), 12.10 (s, 1H, NH), 9.13 (s, 1H, CH=N), 7.71–7.57 (m, 4H, ArH), 7.48–7.38 (m, 3H, ArH), 7.01–6.87 (m, 4H, ArH). ^{13}C NMR (d^6-DMSO, ppm) δ 163.70, 160.89, 157.36, 156.50, 155.75, 151.79, 134.93, 132.62, 131.20, 130.89, 130.80, 129.88, 128.99, 127.56, 122.89, 119.97, 119.72, 118.82, 118.15, 117.93, 115.35. ^{51}V NMR (d^6-DMSO, ppm) δ –553.

2. 5. X-ray Crystallography

Diffraction intensities for the complexes were collected at 298(2) K using a Bruker D8 VENTURE PHOTON diffractometer with Mo*K*a radiation (l = 0.71073 Å). The collected data were reduced using the SAINT program,[9] and multi-scan absorption corrections were performed using the SADABS program.[10] The structures were solved by direct method, and refined against F^2 by full-matrix least-squares method using the SHELXTL.[11] All of the non-hydrogen atoms were refined anisotropically. The coordinated methanol hydrogen atom in **1**·MeOH and the amino hydrogen atom in **2**·H_2O were located from difference Fourier maps and refined isotropically, with O–H and N–H distances restrained to 0.85(1) Å and 0.90(1) Å, respectively. All other hydrogen atoms were placed in idealized positions and constrained to ride on their parent atoms. The crystallographic data for the complexes are summarized in Table 1. Selected bond lengths and angles are given in Table 2. Hydrogen bonding information is listed in Table 3.

Table 1. Crystallographic data and refinement parameters for the complexes

	1·MeOH	**2**·H_2O
Chemical formula	$C_{17}H_{19}ClN_2O_6V$	$C_{21}H_{16}ClFN_3O_7V$
Mr	452.7	527.8
Crystal color, habit	Brown, block	Brown, block
Crystal system	Monoclinic	Monoclinic
Space group	*Cc*	$P2_1/c$
Unit cell parameters		
a (Å)	17.938(1)	7.577(2)
b (Å)	12.072(1)	23.119(3)
c (Å)	10.250(1)	12.393(2)
β (°)	98.617(2)	97.507(2)
V (Å^3)	2194.5(3)	2152.4(6)
Z	4	4
D_{calc} (g cm^{-3})	1.370	1.629
Temperature (K)	298(2)	298(2)
μ (mm^{-1})	0.614	0.644
F(000)	928	1072
Number of unique data	3579	3800
Number of observed data [I > 2σ(I)]	2756	2667
Number of parameters	259	317
Number of restraints	3	4
R_1, wR_2 [$I > 2\sigma(I)$]	0.0656, 0.1666	0.0410, 0.0808
R_1, wR_2 (all data)	0.0890, 0.1833	0.0738, 0.0926
Goodness of fit on F^2	1.046	1.011

Table 2. Selected bond distances (Å) and angles (°) for the complexes

	1		
V(1)–O(1)	1.849(4)	V(1)–O(2)	1.975(4)
V(1)–O(3)	1.580(5)	V(1)–O(4)	1.747(4)
V(1)–N(1)	2.129(5)	V(1)–O(5)	2.289(5)
O(3)–V(1)–O(4)	102.1(2)	O(3)–V(1)–O(1)	100.2(2)
O(4)–V(1)–O(1)	103.2(2)	O(3)–V(1)–O(2)	96.6(2)
O(4)–V(1)–O(2)	93.5(2)	O(2)–V(1)–O(1)	153.1(2)
O(3)–V(1)–N(1)	94.8(2)	O(4)–V(1)–N(1)	160.2(2)
O(1)–V(1)–N(1)	83.6(2)	O(2)–V(1)–N(1)	74.2(2)
O(3)–V(1)–O(5)	175.5(2)	O(4)–V(1)–O(5)	82.1(2)
O(1)–V(1)–O(5)	80.3(2)	O(2)–V(1)–O(5)	81.4(2)
N(1)–V(1)–O(5)	80.8(2)		
	2		
V(1)–O(1)	1.863(2)	V(1)–O(2)	1.942(2)
V(1)–O(3)	2.185(2)	V(1)–O(4)	1.872(2)
V(1)–N(1)	2.081(2)	V(1)–O(6)	1.577(2)
O(6)–V(1)–O(1)	99.2(1)	O(6)–V(1)–O(4)	95.6(1)
O(4)–V(1)–O(1)	107.8(1)	O(6)–V(1)–O(2)	102.0(1)
O(1)–V(1)–O(2)	150.6(1)	O(4)–V(1)–O(2)	90.2(1)
O(6)–V(1)–N(1)	95.8(1)	O(1)–V(1)–N(1)	83.3(1)
O(4)–V(1)–N(1)	162.5(1)	O(2)–V(1)–N(1)	74.5(1)
O(6)–V(1)–O(3)	171.2(1)	O(1)–V(1)–O(3)	81.4(1)
O(4)–V(1)–O(3)	76.0(1)	O(2)–V(1)–O(3)	80.7(1)
N(1)–V(1)–O(3)	93.0(1)		

Table 3. Hydrogen bond distances (Å) and bond angles (°) for the complexes

D*–H···*A	***d*(*D*–H), Å**	***d*(H···*A*), Å**	***d*(*D*···*A*), Å**	**Angle (*D*–H···*A*), °**
1·MeOH				
O(5)–H(5)···O(6)^{i}	0.85(1)	1.79(2)	2.626(7)	166(8)
O(6)–H(6)···N(2)^{ii}	0.82	2.19	2.790(7)	131
2·H_2O				
O(5)–H(5)···O(7)	0.82	1.79	2.607(3)	171
N(3)–H(3)···O(5)	0.90(1)	1.99(3)	2.608(3)	125(3)
N(3)–H(3)···O(4)^{iii}	0.90(1)	2.59(3)	3.310(3)	138(3)
O(7)–H(7A)···O(1)^{iv}	0.85(1)	2.04(2)	2.853(3)	160(4)
O(7)–H(7A)···O(3)^{iv}	0.85(1)	2.61(3)	3.225(3)	131(3)
O(7)–H(7B)···O(6)^{iii}	0.85(1)	2.23(3)	2.808(3)	125(3)
O(7)–H(7B)···N(2)^{v}	0.85(1)	2.47(2)	3.183(3)	142(3)

Symmetry codes: i) *x*, –1 + *y*, *z*; ii) *x*, 1 – *y*, –1/2 + *z*; iii) 1 – *x*, – *y*, 1 – *z*; iv) 2 – *x*, – *y*, 1 – *z*; v) *x*, *y*, –1 + *z*.

3. Results and Discussion

Replacement of two acetylacetonate ligands in [VO(acac)$_2$] by H_2L in methanol resulted in the formation of **1** (Scheme 2). The complex was further reacted with salicylhydroxamic acid to give complex **2** (Scheme 2). The latter complex can also be directly prepared by the reaction of H_2L, salicylhydroxamic acid and [VO(acac)$_2$] in methanol. The V^{IV} in [VO(acac)$_2$] was oxidized to V^{V} by air during the reaction. Both complexes are soluble in DMF, DMSO, methanol, ethanol, and acetonitrile, insoluble in water, chloroform and dichloromethane. Molar conductance of complexes **1** and **2** at the concentration of 10^{-4} M are 17 and 33 Ω^{-1} cm^2 mol^{-1}, respectively, indicating they are non-electrolytes.[12]

3. 1. Crystal Structure Description of 1·MeOH

The molecular structure and atom numbering scheme of complex **1** is shown in Figure 1. The V atom in the com-

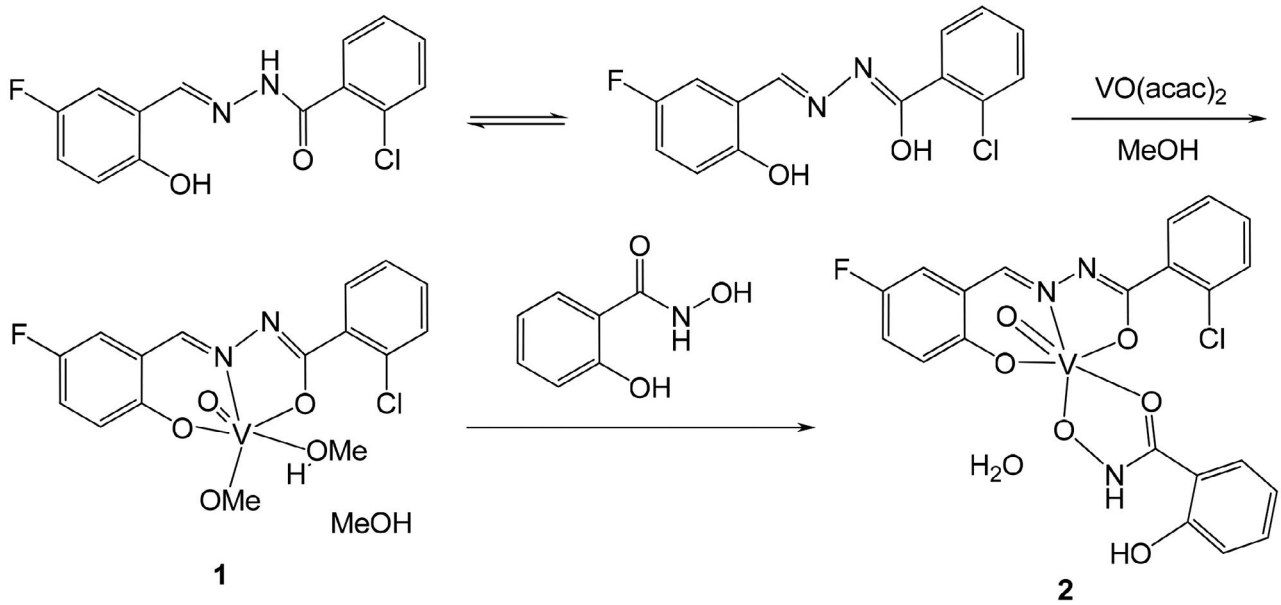

Scheme 2. The synthesis of the complexes

plex is in octahedral coordination, which is coordinated by one oxo oxygen, one neutral and one deprotonated methanol ligands, and the three donor atoms of the doubly deprotonated hydrazone ligand. The neutral methanol ligand is coordinated *trans* to the oxo oxygen, which is similar to those observed in the solvent coordinated vanadium complexes.[3a,4] The vanadium to terminal oxo group (O(3)) bond length for the complex (1.580(5) Å) is within normal range for oxovanadium(V) complexes.[13] The short V(1)–O(3) distance indicates the presence of a vanadium–oxygen double bond.[14] The angular distortion in the octahedral environment around V comes from the five- and six-membered chelate rings taken by the hydrazone ligand, with angles of 83.6(2)° and 74.2(2)°. Distortion of the octahedral coordination can be observed from the coordinate bond angles, ranging from 74.2(2) to 103.2(2)° for the perpendicular angles, and from 153.1(2) to 175.5(2)° for the diagonal angles. Relative to the equatorial plane defined by O(1), O(2), O(4) and N(1), the vanadium atom is displaced toward the axial oxygen atom O3 by 0.291(1) Å. The dihedral angle between the two benzene rings is 83.6(3)°. The double deprotonated form of the hydrazone ligand is consistent with the observed O2–C8 and N2–C8 bond lengths of 1.292(7) Å and 1.302(7) Å, respectively. This is in agreement with reported vanadium complexes containing the enolate form of hydrazone ligands.[4,13b]

In the crystal of **1**, the vanadium complexes are linked by methanol molecules through intermolecular O(5)–H(5)···O(6) and O(6)–H(6)···N(2) hydrogen bonds, to form chains along the *c* axis (Figure 2).

3. 2. Crystal Structure Description of 2·H_2O

The molecular structure and atom numbering scheme of complex **2** is shown in Figure 3. The V atom in the complex is in octahedral coordination, which is coordinated by one oxo oxygen, one hydroxyl and one carbonyl oxygen atoms of SHA ligand, and the three donor atoms of the hydrazone ligand. The carbonyl oxygen atom is coordinated *trans* to the oxo oxygen, with the bond length much longer than the remaining ones. The vanadium to terminal oxo group (O(6)) bond length for the complex (1.577(2) Å) is comparable to that in complex **1**, and within normal range for oxovanadium(V) complexes.[13] The short V(1)–O(6) distance indicates the presence of a vanadium–oxygen double bond.[14] The coordinate bond lengths in the complex are comparable to those observed in **1** and the oxovanadium(V) complexes with octahedral coordination.[4] The angular distortion in the octahedral environment around V comes from the five- and six-membered chelate rings taken by the hydrazone ligand, with angles of 83.34(9)° and 74.47(8)°. Distortion of the octahedral coordination can be observed from the coordinate bond angles, ranging from 74.5(1) to 107.8(1)° for the perpendicular angles, and from 150.6(1) to 171.2(1)° for the diagonal angles. Relative to the equatorial plane defined by O(1), O(2), O(4) and N(1), the vanadium atom is displaced toward the axial oxygen atom O3 by 0.268(1) Å. The dihedral angle between the substituted benzene rings is 21.0(3)°. The double deprotonated form of the hydrazone ligand is consistent with the observed O2–C8 and N2–C8 bond lengths of 1.302(3) Å and 1.297(3) Å, respectively. This is in agreement with reported vanadium complexes containing the enolate form of hydrazone ligands.[4,13b]

In the crystal of **2**, the vanadium complexes are linked by water molecules through intermolecular O(7)–H(7B)···O(6) and O(7)–H(7A)···O(1) hydrogen bonds, to form 1D chains along the *a* axis. The chains are further linked through intermolecular O(5)–H(5)···O(7) and O(7)–H(7A)···O(3) hydrogen bonds in the *c* direction, to form 2D layers (Figure 4).

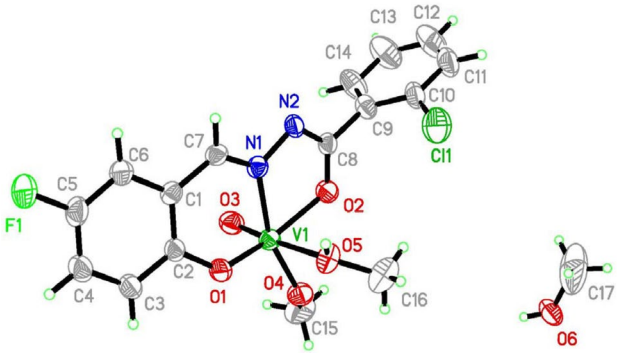

Figure 1. ORTEP plot of the crystal structure of **1**. Displacement ellipsoids of non-hydrogen atoms are drawn at the 30% probability level.

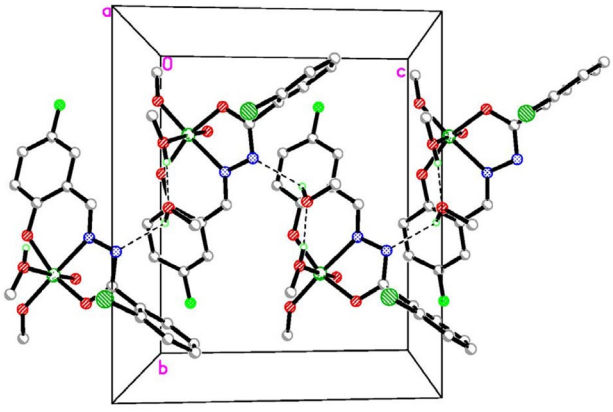

Figure 2. Molecular packing diagram of **1**. Viewed along the *a* axis. Hydrogen atoms not related to hydrogen bonding are omitted. Hydrogen bonds are shown as dashed lines.

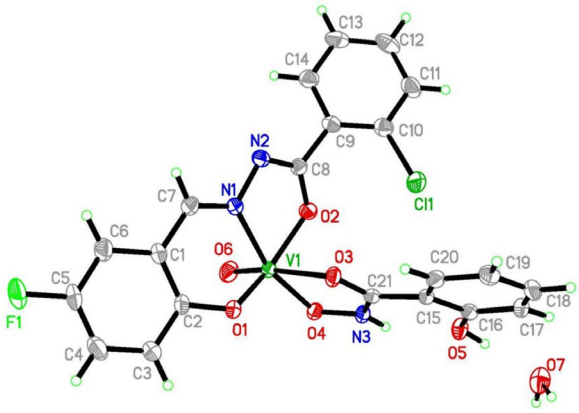

Figure 3. ORTEP plot of the crystal structure of **2**. Displacement ellipsoids of non-hydrogen atoms are drawn at the 30% probability level.

3. 3. IR and Electronic Spectra

The hydrazone ligand showed stretching bands attributed to C=O, C=N, C–OH and NH at about 1651, 1619, 1155 and 1220, and 3232 cm^{-1}, respectively. The complexes exhibit typical bands at about 980 cm^{-1}, assigned to the V=O vibration.[15] In the spectrum of **1**, the bands due to $\nu_{C=O}$ and ν_{NH} were absent, but new C–O stretch appeared at 1253 cm^{-1}. This suggests occurrence of *keto*-imine tautomerization of the hydrazone ligand during complexation. The same phenomenon should occur in complex **2**. But the existence of ν_{NH} at 3278 cm^{-1} made an interruption. The $\nu_{C=N}$ absorption observed at 1619 cm^{-1} in the free hydrazone ligand shifted to 1607 cm^{-1} for both complexes upon coordination to the V atoms.[16] The weak peaks in the low wave numbers in the region 400–650 cm^{-1} may be attributed to V–O and V–N bonds in the complexes.

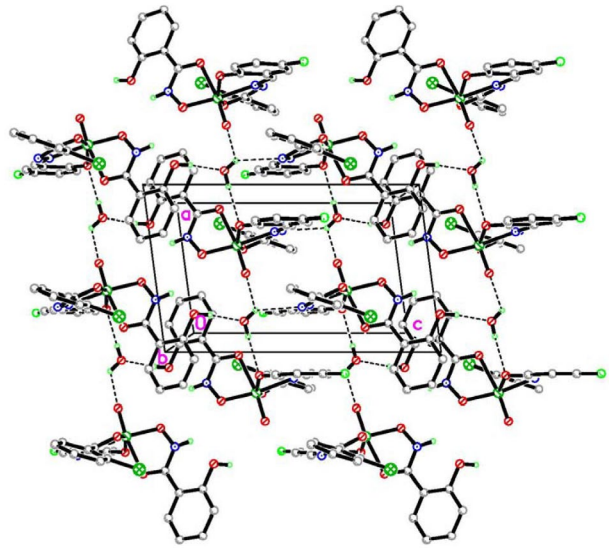

Figure 4. Molecular packing diagram of **2**. Viewed along the *c* axis. Hydrogen atoms not related to hydrogen bonding are omitted. Hydrogen bonds are shown as dashed lines.

Methanol solutions of the complexes are brown-yellow in color. These solutions have been used to record the electronic spectra. The hydrazone ligands and their vanadium(V) complexes have bands in the range 205–240 and 300–330 nm, which can be assigned as $\pi \rightarrow \pi^*$ and $n \rightarrow \pi^*$ transitions, respectively. All bands shift to lower energy in complexes indicating the coordination of ligands to the vanadium ions. The shoulder at about 270 nm for the complexes corresponds to LMCT band of V=O which it is observed at 274 nm for $[VO(acac)_2]$.[14]

3. 4. Thermal Property

Differential thermal and thermal gravimetric analyses were conducted to examine the stability of the complexes. For **1** (Figure 5), the first step started at 50 °C and ended at 160 °C, with a weight loss of 14.0%, might be caused by the loss of the lattice and coordinated neutral methanol molecules. Then the complex continued to decompose, until 470 °C, corresponding to the loss of the remaining parts of the ligands, and formation of V_2O_5. The total weight loss of 78.5% is in agreement with the ideal

value of 79.9%. For **2** (Figure 6), this complex is not very stable in air at room temperature. It might have lost the lattice water molecules before the thermal analysis. The complex started to decompose at 109 °C and completed at 470 °C, corresponding to the loss of the hydrazone and salicylhdroxamate ligands, and formation of V_2O_5. The total weight loss of 83.7% is in agreement with the ideal value of 85.5%.

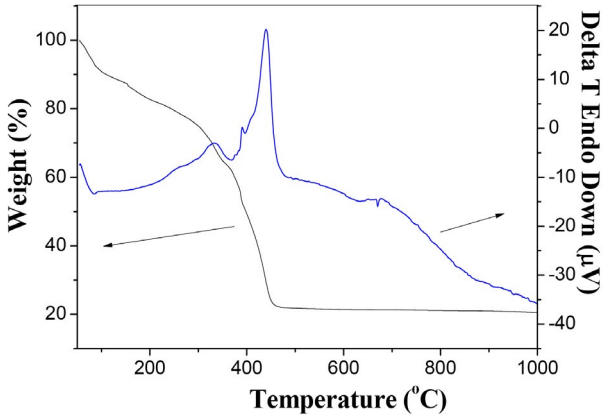

Figure 5. DT-TGA curves of 1.

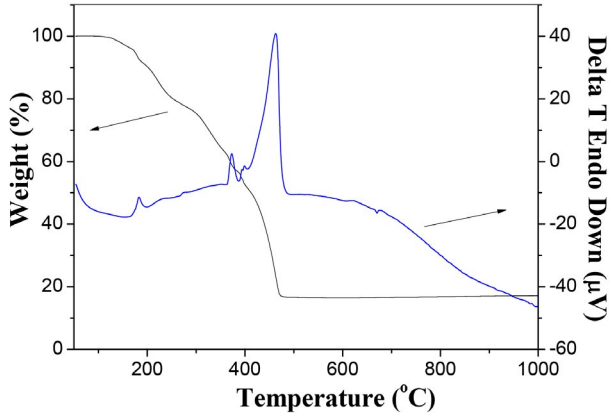

Figure 6. DT-TGA curves of **2**.

3. 5. Antibacterial Activity

The free benzohydrazone and the vanadium complexes were assayed for *in vitro* antibacterial activity against *K. pneumoniae*, *S. aureus*, *P. aeroginosa*, *E. coli*, and *B. subtilis* at 50 μg mL^{-1} using ethanol as solvent and control, and using tetracyclin as the standard drug. The minimum inhibitory concentrations (**MIC**) were determined by broth micro-dilution method.[17] The observed MIC values in μg mL^{-1} are reported in Table 4. The antibacterial activity was evaluated by measuring the zone of inhibition in mm. Ethanol had no antibacterial activity on the bacteria at the concentration studied. The results revealed that the hydrazone compound and the two complexes showed from weak to effective activities against the tested microorganisms. In general, the complexes showed higher activities than the free aroylhydrazones. Such an enhancement in the activity of metal complexes against certain specific microorganisms may be explained on the basis of Overtone's concept and Tweedy's chelation theory.[18] The least MIC with 11 μg mL^{-1} was observed for complex **1** against *S. aureus*. The activity on *B. subtilis* and *S. aureus* of the free hydrazone is less than *N'*-(5-chloro-2-hydroxybenzylidene)-4-hydroxybenzohydrazide (H_2L'), but on *E. coli*, the free hydrazone is higher than the above mentioned compound.[19] The activity of the complexes on *S. aureus* and *E. coli* is similar to the vanadium complex with L' and 2-hydroxybenzoate ligands, while on *B. subtilis*, the complexes are much less than the vanadium complex mentioned above.[19] Thus, more work need to be done to find the relationship between the structures and the antibacterial activities.

4. Supplementary Material

CCDC–978393 for **1** and 978394 for **2** contain the supplementary crystallographic data for this paper. These data can be obtained free of charge at http://www.ccdc.cam.ac.uk/const/retrieving.html or from the Cambridge Crystallographic Data Centre (CCDC), 12 Union Road, Cambridge CB2 1EZ, UK; fax: +44(0)1223-336033 or e-mail: deposit@ccdc.cam.ac.uk.

5. References

1. (a) G. R. Willsky, A. B. Goldfine, P. J. Kostyniak, J. H. McNeill, L. Q. Yang, H. R. Khan, D. C. Crans, *J. Inorg. Biochem.* **2001**, *85*, 33–42; **DOI:**10.1016/S0162-0134(00)00226-9
(b) P. Caravan, L. Gelmini, N. Glover, F. G. Herring, H. L. Li, J. H. McNeill, S. J. Rettig, I. A. Setyawati, E. Shuter, Y. Sun, A. S. Tracey, V. G. Yuen, C. Orvig, *J. Am. Chem. Soc.* **1995**, *117*, 12759–12770; **DOI:**10.1021/ja00156a013
(c) A. Messerschmidt, L. Prade, R. Wever, *Biol. Chem.* **1997**, *378*, 309–315. **DOI:**10.1515/bchm.1997.378.3-4.309

Table 4. Minimum inhibitory concentrations (MICs, μg mL^{-1}) of the compounds

Compound	*K. pneumoniae*	*S. aureus*	*P. aeroginosa*	*E. coli*	*B. subtilis*
H_2L	27	35	> 50	22	36
1	15	11	> 50	17	23
2	17	13	> 50	14	19

2. (a) M. D. Altintop, A. Ozdemir, G. Turan-Zitouni, S. Ilgin, O. Atli, G. Iscan, Z. A. Kaplancikli, *Eur. J. Med. Chem.* **2012**, *58*, 299–307; **DOI:**10.1016/j.ejmech.2012.10.011
(b) X.-L. Wang, Z.-L. You, C. Wang, *J. Chem. Crystallogr.* **2011**, *41*, 621–624; **DOI:**10.1016/j.bmc.2011.04.027
(c) M. A. A. El-Sayed, N. I. Abdel-Aziz, A. A. M. Abdel-Aziz, A. S. El-Azab, Y. A. Asiri, K. E. H. El Tahir, *Bioorg. Med. Chem.* **2011**, *19*, 3416–3424.
3. (a) L. L. Wang, W. Li, Y. J. Mei, *Russ. J. Coord. Chem.* **2019**, *45*, 154–162; **DOI:**10.1134/S1070328419020118
(b) Z.-L. You, D.-H. Shi, J.-C. Zhang, Y.-P. Ma, C. Wang, K. Li, *Inorg. Chim. Acta* **2012**, *384*, 54–61; **DOI:**10.1016/j.ica.2011.11.039
(c) S. Y. Li, W. Q. Zhai, Z. W. Li, A. Li, Y. M. Jiang, W. Li, *Russ. J. Coord. Chem.* **2018**, *44*, 701–706; **DOI:**10.1134/S1070328418110052
(d) Z.-L. You, Y.-M. Cui, Y.-P. Ma, C. Wang, X.-S. Zhou, K. Li, *Inorg. Chem. Commun.* **2011**, *14*, 636–640. **DOI:**10.1016/j.inoche.2011.01.038
4. (a) N. A. Lalami, H. H. Monfared, H. Noei, P. Mayer, *Transition Met. Chem.* **2011**, *36*, 669–677; **DOI:**10.1007/s11243-011-9517-8
(b) T. N. Mandal, S. Roy, A. K. Barik, S. Gupta, R. J. Butcher, S. K. Kar, *Polyhedron* **2008**, *27*, 3267–3274. **DOI:**10.1016/j.poly.2008.07.024
5. S. Gao, Z.-Q. Weng, S.-X. Liu, *Polyhedron* **1998**, *17*, 3595–3606. **DOI:**10.1016/S0277-5387(98)00154-5
6. S. P. Rath, K. K. Rajak, S. Mondal, A. Chakravorty, *J. Chem. Soc. Dalton Trans.* **1998**, 2097–2101. **DOI:**10.1039/a801355a
7. M. Sutradhar, T. R. Barman, G. Mukherjee, M. G. B. Drew, S. Ghosh, *Polyhedron* **2012**, *34*, 92–101. **DOI:**10.1016/j.poly.2011.12.022
8. M. Zhang, D.-M. Xian, H.-H. Li, J.-C. Zhang, Z.-L. You, *Aust. J. Chem.* **2012**, *65*, 343–350. **DOI:**10.1071/CH11424
9. Bruker, SMART and SAINT, Bruker AXS Inc., Madison, Wiscon sin, USA, **2012**.
10. G. M. Sheldrick, SADABS Program for Empirical Absorption Correction of Area Detector, University of Göttingen, Germany, **1996**.
11. G. M. Sheldrick, *Acta Crystallogr.* **2008**, *A64*, 112–122. **DOI:**10.1107/S0108767307043930
12. W. J. Geary, *Coord. Chem. Rev.* **1971**, *7*, 81–122. **DOI:**10.1016/S0010-8545(00)80009-0
13. (a) M. R. Prathapachandra Kurup, E. B. Seena, M. Kuriakose, *Struct. Chem.* **2010**, *21*, 599–605; **DOI:**10.1007/s11224-010-9589-7
(b) Y. Li, L. Xu, M. Duan, J. Wu, Y. Wang, K. Dong, M. Han, Z. You, *Inorg. Chem. Commun.* **2019**, *105*, 212–216. **DOI:**10.1016/j.inoche.2019.05.011
14. H. H. Monfared, R. Bikas, P. Mayer, *Inorg. Chim. Acta* **2010**, *363*, 2574–2583. **DOI:**10.1016/j.ica.2010.04.046
15. S. Guo, N. Sun, Y. Ding, A. Li, Y. Jiang, W. Zhai, Z. Li, D. Qu, Z. You, *Z. Anorg. Allg. Chem.* **2018**, *644*, 1172–1176. **DOI:**10.1002/zaac.201800060
16. H. Yu, S. Guo, J.-Y. Cheng, G. Jiang, Z. Li, W. Zhai, A. Li, Y. Jiang, Z. You, *J. Coord Chem.* **2018**, *71*, 4164–4179. **DOI:**10.1080/00958972.2018.1533959
17. J. H. Jorgensen, J. D. Turnidge, Manual of Clinical Microbiology, Washington (DC, USA): American Society for Microbiology, 2003.
18. (a) N. Dharamaraj, P. Viswanathamurthi, K. Natarajan, *Transition Met. Chem.*, **2001**, *26*, 105–109; **DOI:**10.1023/A:1007132408648
(b) J. W. Searl, R. C. Smith, S. Wyard, *J. Proc. Phys. Soc.*, **1961**, *78*, 1174–1181. **DOI:**10.1088/0370-1328/78/6/311
19. C. Li, Y.-L. Dong, X.-F. Meng, X. Zhou, J.-J. Ma, *Synth. React. Inorg. Met.-Org. Nano-Met. Chem.*, **2016**, *46*, 118–122. **DOI:**10.1080/15533174.2014.900791

Povzetek

Nov vanadijev(V) kompleks, [VOL(OMe)(MeOH)]·MeOH (**1**·MeOH), smo pripravili z reakcijo $VO(acac)_2$ z 2-kloro-*N*'-(5-fluoro-2-hidroksibenziliden)benzohidrazidom (H_2L) v metanolu. Z dodatkom salicilhidroksamske kisline (HSHA) k metanolni raztopini **1**, smo izolirali nov salicilhidroksamato vanadijev(V) kompleks, [VOL(SHA)]·H_2O (**2**·H_2O). Oba kompleksa smo okarakterizirali z elementno analizo, infrardečo spektroskopijo, termično analizo in rentgensko monokristalno analizo. Kompleks **1** kristalizira z molekulo metanola kot solvatom in kompleks **2** kot hidrat. V kompleksih so V atomi oktaedrično koordinirani. V kristalni strukturi **1**·MeOH so vanadijevi kompleksi povezani z molekulo metanola preko intramolekularnih O–H···N in O–H···O vodikovih vezi v verige vzdolž osi *c*. V kristalni strukturi **2**·H_2O so vanadijevi kompleksi povezani z molekulo vode preko intermolekularnih O–H···O vodikovih vezi v verige vzdolž osi *a*. Nadalje so verige povezane v plasti preko intermolekularnih intermolekularnih O–H···N in O–H···O vodikovih vezi vzdolž osi *c*. Določili smo tudi antimikrobno aktivnost obeh kompleksov proti *K. pneumoniae*, *S. aureus*, *P. aeroginosa*, *E. coli* in *B. subtilis*.